Experimental printed circuit steam generator design for dryout induced thermal fatigue study

Jin Su Kwon[a], Sung Gil Shin[a], Jeong Ik Lee[a,*], Sang Ji Kim[b]
[a]*Department of Nuclear and Quantum Engineering, Korea Advanced Institute of Science and Technology, 373-1 Guseong-dong Yuseong-gu,Daejeon 305-701, Republic of Korea*

[b]*Korea Atomic Energy Research Institute*
150 Dukjin-dong, Yuseong-gu, Daejon 305-353, Republic of Korea

[*]*Corresponding author: jeongiklee@kaist.ac.kr*

1. Introduction

Attaching compact steam generators to Small Modular Reactors (SMR) has become an area of interest. Especially, printed circuit steam generators (PCSG), a kind of printed circuit heat exchanger (PCHE) designed for the steam generator application, have been studied as a potential candidate for the steam generator in SMART, a small-sized integral-type PWR developed at KAERI in Korea [1, 2]. The schematic diagram of the PCHE is shown in Figure 1. Outstanding structural rigidity comes from the nature of the manufacturing process. PCSG is fabricated by stacking multiple chemical-etched plates and diffusion bonded together under high temperature and pressure. A huge heat transfer area with the micro-sized semi-circular channels make PCSG significantly compact. This makes it a promising technology for the SMART reactor.

SMART development group has introduced a once-through steam generator by taking into account the spatial constraints and operational requirements of the steam generator installed inside the reactor. Thus, PCSG is operated in the boiling regimes including nucleate boiling, dryout, and vapor film boiling to produce superheated steam. The dryout occurs where the liquid film in contact with the heated wall disappears and enters the vapor film boiling region. The movement of dryout front, which is caused by unstable nature regardless of density wave oscillation, induces a transition in boiling regimes between nucleate boiling and vapor film boiling regimes [3]. It leads to a significant wall temperature oscillation that has a detrimental effect on the component life due to cyclic thermal stresses. Hence, thermal oscillations induced by dryout should be studied to determine the component integrity and service lifetime.

This type of oscillation was studied in shell and tube steam generators [4]. Most previous studies have been conducted on macro-sized tubes. Studies on micro-sized tubes are very limited. Accordingly, the frequency of wall temperature oscillation at the dryout front in semi-circular micro-sized channel should be studied through experiments. The purpose of this study is to investigate the major parameters and the value of each parameter to determine the test matrix of the experiment.

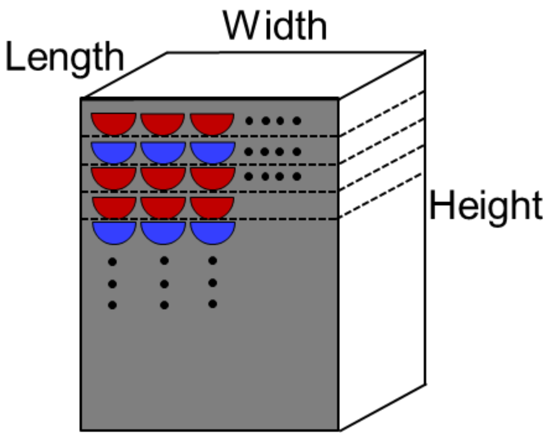

Figure 1. Schematic diagram of the PCHE block

2. Methods and Results

2.1 Major parameters of thermal oscillations

Since the steam generators in SMART produce superheated steam, there will be a point where dryout occurs inside the heat transfer channel. However, since attachment and detachment of liquid film will rapidly occur at the dryout point, it is natural to assume that the heat transfer channel wall will experience significant thermal fatigue over the service lifetime. Samra et al. described that the thermal oscillation period in macro-sized tubes can be represented as the following 7 variables containing the abovementioned parameters [5].

$$t_p = f\left(x_d, g, \rho_l, \rho_v, (\rho_l - \rho_v) g, \sigma, D\right) \quad (1)$$

In the experiments, it is appropriate to use heat flux instead of quality for the experimentally controlled variable due to better controllability. Thermodynamic variables such as density and surface tension can be captured by controlling pressure. In this study, a simulant of water will be used for the experiment to reduce the experiment cost while studying the effect of thermodynamic properties. The simulant fluid will be most likely to be a refrigerant and it will be selected in the next step of research.

The major parameters that consist the experimental matrix were decided as mass flux, heat flux, channel diameter, and working fluid. In the next section, the range of values for test will be studied through the PCSG design for SMART.

2.2 Steam generator design scheme

The existing heat exchanger analysis methods such as the log mean temperature difference method (LMTD) may not be the best method in evaluating the thermal performance of steam generators due to significant heat transfer coefficient variation in the two-phase regime.

To resolve the change of heat transfer coefficient inside the heat exchanger, a PCSG analysis tool was developed based on the 1-D finite difference method. The heat transfer in each control volume can be obtained by thermal resistance networks.

$$Q = UA\Delta T = \frac{1}{\frac{1}{h_{hot}A} + \frac{t}{h_{conduction}A} + \frac{1}{h_{cold}A}}\Delta T \tag{2}$$

The pressure drop in the control volume is calculated considering frictional and acceleration term as following equations.

$$\Delta P_{fric,i} = f_i \frac{L}{D_e}\frac{\rho_i v_i^2}{2} \tag{3}$$

$$\Delta P_{acceleration,i} = G^2\left[\frac{x_i^2}{\rho_g\alpha_i} + \frac{(1-x_i)^2}{\rho_f(1-\alpha_i)} - \frac{x_{i-1}^2}{\rho_g\alpha_{i-1}} - \frac{(1-x_{i-1})^2}{\rho_f(1-\alpha_{i-1})}\right] \tag{4}$$

Hence, the thermodynamic properties can be obtained from the heat transfer and pressure drop of the previous control volume. The calculation above is carried out sequentially from the inlet to the outlet. The hot side outlet thermodynamic properties are assumed first to calculate the first control volume corresponding to the cold side inlet since most of the steam generators are designed as a counter-current type. The numerical iterations using the secant method are performed to ensure that the hot side inlet temperature and pressure from the calculation are equal to the initial assumptions. The steam generator analysis flow diagram is shown in Figure 2. This approach is well validated with the results of the KAIST experimental facility when using water as a working fluid [6]. Accordingly, the results of this scheme with 400 control volumes are used as the reference data.

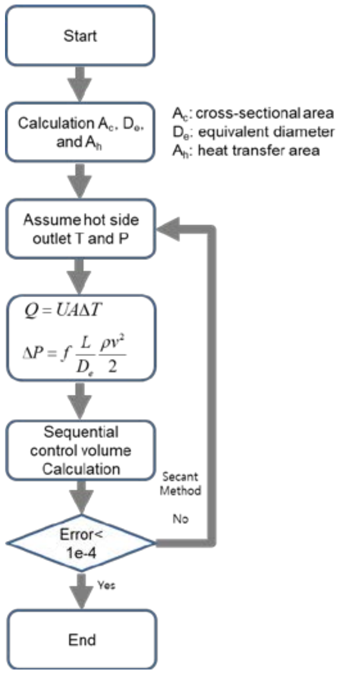

Figure 2. Flow chart of heat exchanger design scheme

2.3 Implemented correlations

Correlations were mostly adopted from the nuclear system analysis code TRACE developed by U.S.NRC. The TRACE theory manual contains various correlations and the reasons for adoption. More detailed information is provided in the TRACE theory manual [7].

In the primary system, the flow regime is maintained in the liquid single phase. The Gnielinski correlation, which is generally used in the regime, is applied and the friction factor in Gnielinski correlation is evaluated by Filonenko's formula. The correction factor for temperature-dependent property effects for single-phase liquid heat transfer is introduced in TRACE. When it comes to the frictional factor, the Churchill formula was used since it applies to all three flow regimes - laminar, transition, and turbulent.

In the secondary system, the steam generator for SMART experiences boiling regimes including nucleate boiling, dryout, and dispersed film boiling since it is designed to produce superheated steam. Thus, two-phase correlations at each boiling regimes were implemented considering void fraction and occurrence of dryout. It is noted that two-phase correlations from TRACE are studied under the macro-sized circular tube. These may not be suitable for the micro-sized semi-circular channels typical to PCSGs. Since there is little information about the semi-circular channel, this study attempts to give an overview of the characteristics of the PCSG by applying existing correlations. The correlations, which are applied to the steam generator design scheme, are summarized in Tables I and II.

2.4 Design condition of the steam generator

Design conditions of the SMART steam generator were obtained from Kang et al.'s study [2]. The inlet temperature, pressure, and mass flow rate are fixed for this study. The mass flow rate of the cold side is significantly small compared to the hot side mass flow rate because the heat transfer is mainly carried out by the latent heat on the cold side. In order to compare the size of the heat exchanger, the same heat duty and pressure drop constraints were given. The pressure drop of 85 kPa was used in the secondary side, which is different from the reference. This is because secondary side PCSG plates have a section for merging and dividing working fluid between channels in the reference, while that is not considered in this paper.

When designing the PCSG, channel diameter is the same on the hot and cold sides for ease of fabrication. The number of channels on the hot side is fixed to twice the number of channels on the cold side to match the pressure drop between both sides. The configuration of PCSG is shown in Figure 1. The channel geometry was determined as a straight type to evaluate the heat exchanger with existing correlations. The optimized heat exchanger can be obtained by adjusting the geometry parameters such as channel diameter, channel length, and the number of channels to match the target heat duty and pressure drop. After calculating the heat exchanger volume using the channel length and number, approximate geometry information was obtained assuming that the width and height of the PCSG block are the same.

2.5 PCSG design results

The sensitivity study of PCSG, which is presented in Figure 3, shows that the volume of the steam generator is minimized when the channel diameter is 1.5 mm under the same heat duty and pressure drop condition. The volume of the steam generator becomes smaller until it reaches the optimum diameter as the channel diameter decreases due to increased heat transfer area. When the channel diameter is less than 1.5 mm, the width and height of the PCHE block are considerably larger than the channel length, so the volume of the steam generator increases. One consideration in PCSG design is manufacturability. The maximum plate width and height are considered 60 cm because of the limited capability of the furnace for diffusion bonding [8]. Accordingly, the channel diameter of PCSG for SMART was chosen as 2 mm in consideration of manufacturability and potential fouling effects in this study. The number of channels on the hot and cold sides is 32,000 and 16,000, respectively, and the mass flux on the cold side is 533 kg/m^2-sec. The designed PCSG volume is almost one-thirtieth of the existing helical type steam generator [2]. It indicates that PCSG is definitely an attractive candidate for the steam generator in the view of compactness.

Each heat transfer regime can be intuitively distinguished by the temperature profile inside the PCSG as shown in Figure 5. It can be seen that the cold side wall temperature rises rapidly due to dryout at the HX location near 0.55m. Dryout occurred when the heat flux was 760 kW/m^2, and heat transfer deteriorated immediately, resulting in heat flux of 220 kW/m^2. Consequently, the test matrix is planned to include a mass flux of 530 kg/m^2-sec and a heat flux of 760 kW/m^2. Considering the possibility that PCSG can be designed in different channel shapes, the diameter effect will be studied by testing with 2, 3, and 4mm diameter channels.

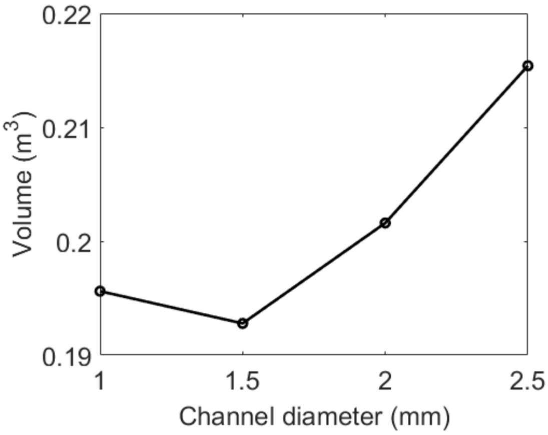

Figure 3. PCSG volume versus channel diameter

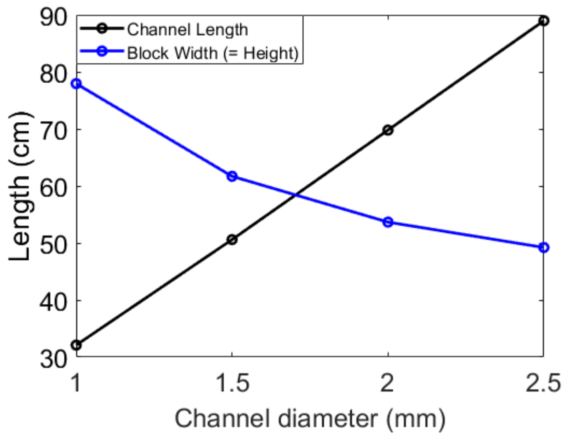

Figure 4. Length and the width (= height) versus channel diameter

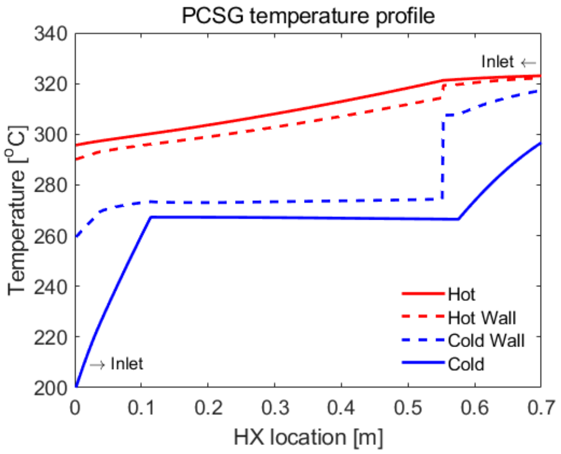

Figure 5. Temperature profile inside the designed PCSG

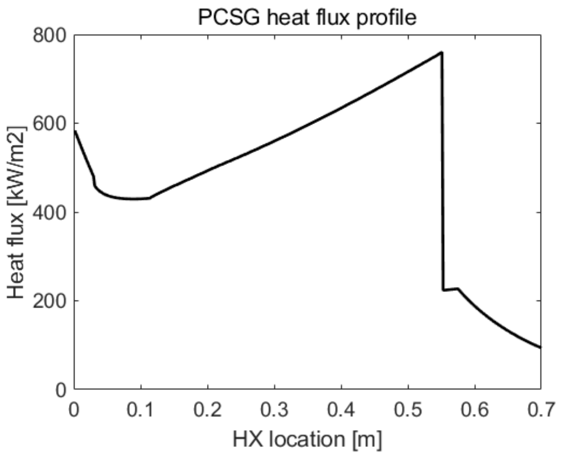

Figure 6. Heat flux profile inside the designed PCSG

3. Summary and conclusions

A printed circuit heat exchanger type steam generator is considered for the future SMRs. If an SMR produces superheated steam, dryout will occur in the steam generator, and evaluation of thermal fatigue induced by dryout in PCSG is not evaluated in detail previously. Thus, an experiment was planned to take place to understand the phenomena. The major experimentally controlled parameters were chosen as mass flux, heat flux, diameter, and working fluid from the literature survey. To determine the test conditions for the experiment, a preliminary sizing of PCSG for SMART was performed in this study. For the further study, the experimental apparatus will be designed and constructed to conduct the test.

ACKNOWLEDGEMENTS

This work was supported by the National Research Foundation of Korea (NRF) grant funded by the Korean Government (MIST). (No. 2018M2A8A4081307)

REFERENCES

[1] Shin, Chang Wook, and Hee Cheon No. "Experimental study for pressure drop and flow instability of two-phase flow in the PCHE-type steam generator for SMRs." *Nuclear Engineering and Design* 318 (2017): 109-118.
[2] Han-Ok Kang, Hun Sik Han, Young-In Kim, Keung Koo Kim, Thermal Sizing of Printed Circuit Steam Generator for Integral Reactor, Transactions of the Korean Nuclear Society Spring Meeting, Jeju, Korea, May 29-30, 2014
[3] Chiang, T., D. M. France, and T. R. Bump. "Calculation of tube degradation induced by dryout instability in sodium-heated steam generators." *Nuclear Engineering and Design* 41.2 (1977): 181-191.
[4] France, D. Mo, et al. "Characteristics of transition boiling in sodium-heated steam generator tubes." *Journal of Heat Transfer* 101.2 (1979): 270-275.
[5] Samra, S. S., and V. K. Dhir. "Study of thermal oscillations at the dryout front in half heated tubes." *Journal of solar energy engineering* 107.4 (1985): 343-351.
[6] Baik, Seungjoon, et al. "Study on CO2–water printed circuit heat exchanger performance operating under various CO_2 phases for S-CO_2 power cycle application." Applied Thermal Engineering 113 (2017): 1536-1546.
[7] NRC, US. "TRACE V5. 0 Theory Manual, Field Equations, Solution Methods, and Physical Models." United States Nucl. Regul. Comm (2010).
[8] Kim, I.H., “Experimental and Numerical Investigations of Thermal-hydraulic Characteristics for the Design of a Printed Circuit Heat Exchanger (PCHE) in HTGRs,” Doctoral dissertation, Korea Advanced Institute of Science and Technology, 2012.

Table I: Summarized heat transfer correlations for the steam generator design scheme

Single-phase	Water	TRACE - Gnielinski $Nu=\frac{(f/8)(\mathrm{Re}-1000)\mathrm{Pr}}{1+12.7(f/8)^{0.5}(\mathrm{Pr}^{2/3}-1)}\times\left(\frac{\mathrm{Pr}_l}{\mathrm{Pr}_w}\right)^{0.11}$ $f=\left(0.79\ln(\mathrm{Re})-1.64\right)^{-2}$
	Steam	TRACE - Gnielinski $Nu=\frac{(f/8)(\mathrm{Re}-1000)\mathrm{Pr}}{1+12.7(f/8)^{0.5}(\mathrm{Pr}^{2/3}-1)}\times\left(\frac{T_w}{T_v}\right)^{n}$ $f=\left(0.79\ln(\mathrm{Re})-1.64\right)^{-2}$ $n=-\left(\log_{10}(T_w/T_v)\right)^{0.25}+0.3$
Two-phase	ONB	MARS-KS $T_{ONB}=T_{sat}-0.001$
	Nucleate boiling	TRACE
	CHF	CHF lookup table 2006
	Inverted annular film boiling (Void fraction < 0.6)	TRACE
	Inverted slug film boiling (0.6 < Void fraction < 0.9)	TRACE
	Dispersed flow film boiling (0.9 < Void fraction < 1)	TRACE
	Void fraction	Lockhart-Martinelli $X^2=\left(\frac{\mu_f}{\mu_g}\right)^{0.2}\left(\frac{x_f}{x_g}\right)^{1.8}\left(\frac{\rho_g}{\rho_f}\right)$ $\alpha=1-\frac{X}{\left(1+20X+X^2\right)^{0.5}}$

Table II: Summarized frictional factor correlations for the steam generator design scheme

Single-phase		TRACE - Churchill $f_w=2\left[\left(\frac{8}{\mathrm{Re}}\right)^{12}+\frac{1}{(a+b)^{3/2}}\right]^{1/12}$ $a=\left\{2.457\ln\left[\frac{1}{\left(\frac{7}{\mathrm{Re}}\right)^{0.9}+0.27\left(\frac{\varepsilon}{D_h}\right)}\right]\right\}^{16}$ $b=\left(\frac{3.753\times10^4}{\mathrm{Re}}\right)^{16}$
Two-phase	Bubbly/Slug flow (Void fraction < 0.8)	TRACE
	Transition from bubbly/slug to annular (0.8 < Void fraction < 0.9)	TRACE
	Annular flow (0.9 < Void fraction < 1)	TRACE